

APPLICATION OF SIMPLE MODELS TO THE STUDY OF NONEQUILIBRIUM BEHAVIOUR OF INELASTIC GASES

UMBERTO MARINI BETTOLO MARCONI^{a,*},
ANDREA PUGLISI^b and ANDREA BALDASSARRI^c

^a*Dipartimento di Fisica, Università di Camerino and Istituto Nazionale di Fisica della Materia,
Via Madonna delle Carceri, 62032 Camerino, Italy;*

^b*Laboratoire de Physique Théorique Unité Mixte de Recherche UMR 8627, Bâtiment 210,
Université de Paris-Sud, 91405 Orsay Cedex, France;*

^c*Dipartimento di Fisica, Università La Sapienza and INFN Unità di Roma I,
P.le A. Moro 2, 00185 Rome, ITALY*

(Received 27 December 2003)

The dynamics of cooling inelastic gases and the evolution of their velocity fields is addressed by studying a series of simplified models. We first discuss a model of inelastic hard particles, which shows an uncorrelated transient phase (homogeneous cooling state or Haff regime) followed by the emergence of structures in the velocity and density field. Motivated by the linear stability analysis of the Haff regime, which predicts the appearance of density clusters only *after* the formation of structures in the velocity field, we focus our attention on the velocities of the gas particles. We study the so-called inelastic Maxwell model (IMM), first in a version with infinite connectivity which is the analog of mean-field spin systems. Secondly, we embed the model onto a lattice (in one dimension and two dimension), in order to observe spatial correlations. The mean-field IMM has the advantage that it lends itself to analytical treatment: in one dimension we find an exact asymptotic scaling solution for the probability density function (p.d.f.) of velocities. On the other hand, the lattice version displays typical spatial features of an inelastic gas, e.g., the transient Haff regime followed by the coarsening of structures in the velocity field (shocks in one dimension, vortices and shocks in two dimension), the so-called “return to the Gaussian” phenomenon of the velocity p.d.f. observed in MD simulations, etc. We show that the growth of structures in the lattice model is similar to that of domains in a diffusive field, but presents a short-scale disorder (“internal noise”) which is induced by the randomizing effect of collisions. In the lattice model, we can also establish the presence or absence of a mesoscopic scale which is required for a hydrodynamics description of the field evolution.

Keywords: Inelastic gas; Granular materials; Inelastic Maxwell model; Lattice model

1. INTRODUCTION

Deriving the laws which govern the macroscopic behaviour of many-particle systems far from thermal equilibrium is one of the main tasks of statistical physics and is currently a subject of active study. Whereas equilibrium phenomena are rather well

*Corresponding author. E-mail: umberto.marini.bettolo@roma1.infn.it

understood, a general framework for studying nonequilibrium phenomena is still not available. The main obstacle to such a comprehension is the difficulty of combining the statistical and dynamical descriptions. Hence, the study of specific models is mandatory since it seems reasonable that the general picture will appear only by comparing the behaviour of different systems driven out of equilibrium by varying an external field, such as pressure or temperature. According to the particular conditions under which an experiment is conducted, the system may or may not reach a steady state. Fluids undergoing phase separation, or the ordering of magnetic materials, are examples of familiar and well-studied nonequilibrium processes (Bray, 1994).

More recently, there has been a surge of interest toward a different nonequilibrium system, represented by a granular gas, i.e., an assembly of macroscopic particles, which can be described as many-body systems with strongly repulsive and energy nonconserving interactions. This system shows rather peculiar and intriguing features both with respect to its static and dynamical properties. A dilute granular system, subject to tapping, shaking or some other kind of external driving, which supplies the energy dissipated by the inelastic collisions, may have a behaviour resembling that of a standard fluid, but with interesting peculiarity. On the other hand, in the absence of external forces it gradually loses its kinetic energy and comes to rest. In addition, it may become spontaneously inhomogeneous and form patterns. Such a behaviour, typical of the free cooling process, displays interesting analogies and connections with other areas of nonequilibrium statistical mechanics such as ordering kinetics (Bray, 1994), decaying turbulence (Frisch and Bec, 2001), etc. A gas of inelastic hard spheres (IHS), due to its relative simplicity, represents a standard reference model for fluidized granular materials (Goldhirsch and Zanetti, 1993; Pöschel and Luding, 2000). Many of its properties are well understood. In particular, a great deal of attention was devoted to the study of the cooling process that occurs when an assembly of grains, initially in motion, evolves in the absence of any external energy feed.

Dilute granular flows can be described by including the presence of inelastic interactions in the formalism of the Boltzmann equation, which governs the evolution of the one-particle distribution function taking into account only binary collisions. However, since the solutions of the Boltzmann equation, which is a nonlinear integro-differential equation, are not known for an arbitrary choice of the inter-particle potential and of the boundary conditions, one has to resort either to approximations, numerical solutions or alternatively to simplified models. In some of these simplified models, it is possible to obtain closed solutions or at least a significant reduction of the numerical effort.

The first example of such an attitude is represented by the attention dedicated to the so-called Maxwell molecules. By an appropriate choice of the intermolecular potential the collision rate becomes a simple function of the energy and the resulting Boltzmann equation greatly simplifies. Several important studies have dealt with the treatment of the Boltzmann equation for Maxwell molecules (see review (Ernst, 1981)), i.e., of energy conserving systems. Among these, perhaps the most influential has been the work of Bobylev (1975) and independently of Krook and Wu (1976, 1977), who found exact similarity solutions for the model. After a period of relative calm, the advent of granular systems has revived the interest toward Maxwell models (Ben-Naim and Krapivsky, 2000). In the case of inelastic systems, in order to justify the major simplicity of the Boltzmann equation, one cannot invoke a particular form of the inter-particle potential, but has to assume its form as a definition. Nevertheless, the model displays

a behaviour which parallels that of more realistic systems, but also shows statistical features of great interest.

Inelastic Maxwell models are studied in the present article both in the absence of spatial coordinates (homogeneous inelastic Maxwell model) and embedded onto a lattice, in order to recover the information on the evolution of spatial structures, which is one of the most outstanding features of experiments and theory in granular gases. Our aim is to show that these models have properties that are interesting in a context that is more general than granular physics. In particular, the results on the homogeneous model are of importance for the general theory of Boltzmann equations, while the lattice version is a rich and simple model which displays ordering kinetics features with nontrivial peculiarities. However our starting point is the granular gas prototype, i.e., the gas of inelastic hard particles, and most of our results are compared with its properties, which are known from theory and numerical simulations.

2. THE MODEL OF INELASTIC HARD PARTICLES

Granular gases are defined, in the present article, as assemblies of inelastic hard objects, i.e., particles that interact by means of instantaneous binary collisions. The inelasticity is accounted through the so-called normal restitution coefficient, $\alpha \in [0, 1]$, which measures the fraction of normal relative velocity (i.e., the component parallel to the line joining the centres of the colliding particles) which is conserved after the collision. When $\alpha < 1$ the gas is inelastic, energy is non-conserved and, most noticeably, the velocities of the particles after the collision result *more parallel* than before the collision. This is the mechanism that induces ordering at the microscopic level.

Let us consider a system of volume V containing N particles in d dimensions, which perform rectilinear trajectories between collision events. When a pair collides a fraction of the total kinetic energy is dissipated, but the total momentum is conserved. The post-collisional velocities ($\mathbf{v}_1^*, \mathbf{v}_2^*$) are determined by the transformation:

$$\mathbf{v}_1^* = \mathbf{v}_1 - \frac{1}{2}(1 + \alpha)(\mathbf{v}_{12} \cdot \hat{\boldsymbol{\sigma}})\hat{\boldsymbol{\sigma}}, \quad (1)$$

where $\mathbf{v}_{12} = \mathbf{v}_1 - \mathbf{v}_2$, $\hat{\boldsymbol{\sigma}}$ is a unit vector along the line of centres of the colliding spheres at contact and α is the coefficient of restitution.

If an isolated granular gas is initially prepared in a state in which the density is uniform and the velocities have a Maxwellian distribution, it will rapidly dissipate its internal energy under the effect of the mutual inelastic collisions. The system evolving from a homogeneously random state loses memory of its initial condition after a time of the order of one collision per particle and rapidly enters the so-called homogeneous cooling state (HCS). In this regime, in the low density limit, the temporal evolution of the one-particle distribution function is described by the Boltzmann inelastic equation (see for example van Noije and Ernst, 1998a). Under the molecular chaos hypothesis we have

$$(\partial_t + \mathbf{v} \cdot \nabla)f(\mathbf{r}, \mathbf{v}, t) = I(f, f), \quad (2)$$

where $I(f, f)$ is the inelastic Boltzmann collision operator. In the case of IHS one obtains an explicit representation of the collision integral (van Noije and Ernst, 1998b):

$$I(f, f) = \sigma^{d-1} \int d\mathbf{v}_2 \int' d\hat{\boldsymbol{\sigma}} (\mathbf{v}_{12} \cdot \hat{\boldsymbol{\sigma}}) \left\{ \frac{1}{\alpha^2} f(\mathbf{v}_1^{**}, t) f(\mathbf{v}_2^{**}, t) - f(\mathbf{v}, t) f(\mathbf{v}_2, t) \right\}. \quad (3)$$

The prime on the $\hat{\boldsymbol{\sigma}}$ integration enforces the condition $\mathbf{v}_{12} \cdot \hat{\boldsymbol{\sigma}} > 0$, where \mathbf{v}_i^{**} represent the precollisional velocities, which are functions of \mathbf{v} and \mathbf{v}_2 and can be computed by inversion of Eq. (1).

In the HCS, the system displays uniform density and kinetic temperature and a vanishing coarse-grained velocity field. The kinetic definition of HCS is given by the homogeneity ansatz plus the scaling ansatz for the one-particle distribution function:

$$f(\mathbf{r}, \mathbf{v}, t) = \frac{n}{v_0^d(t)} p(\mathbf{c}), \quad (4)$$

where $\mathbf{c} = \mathbf{v}/v_0(t)$ and $v_0(t)$ is the thermal velocity defined by $T(t) = mv_0^2(t)/d$ with $T(t)$ the granular temperature; here we have assumed that $\int d\mathbf{c} p = 1$.

In order to obtain the evolution equation for the granular temperature

$$T(t) = \frac{1}{d} \frac{m}{n} \int d\mathbf{v} v^2 f(\mathbf{v}, t) = \frac{1}{2} m v_0^2(t), \quad (5)$$

where m is the particle mass and $n = N/V$, we multiply both sides of Eq. (2) by $m\mathbf{v}_1^2$ and integrate over coordinate and velocity space. This yields

$$\frac{dT(t)}{dt} = -\frac{2}{d} n \mu_2 \sigma^{d-1} v_0 T(t) = -2\gamma \omega T(t), \quad (6)$$

where, following (van Noije and Ernst, 1998b), the nondimensional quantity μ_2 is defined as:

$$\mu_2 = -\frac{1}{v_0^3} \frac{1}{n^2} \int d\mathbf{v}_1 v_1^2 I(f, f). \quad (7)$$

The Enskog collision frequency, ω , for inelastic hard spheres is

$$\omega = \frac{\Omega_d}{\sqrt{2\pi}} n \sigma^{d-1} v_0, \quad (8)$$

and the nondimensional spontaneous cooling rate, γ , is

$$\gamma = \frac{\sqrt{2\pi}}{d\Omega_d} \mu_2, \quad (9)$$

where $\Omega_d = 2\pi^{d/2}/\Gamma(d/2)$ is the surface area of a d -dimensional unit sphere.

To proceed further analytically, one assumes the distribution function to be a Maxwellian:

$$f_M(\mathbf{v}, t) = \frac{n}{(2\pi T)^{d/2}} \exp\left(-\frac{\mathbf{v}^2}{2T}\right). \quad (10)$$

In this case, by solving the integrals, we obtain:

$$\gamma = \frac{(1 - \alpha^2)}{2d}, \quad (11)$$

so that the temperature equation reads:

$$\frac{dT(t)}{dt} = -\frac{(1 - \alpha^2)}{d} \omega T(t). \quad (12)$$

By introducing the nondimensional time variable τ , representing the average number of collisions experienced per particle in a time t , and defined through $d\tau = \omega[T(t)] dt$, we obtain

$$T(\tau) = T(0) \exp(-2\gamma\tau), \quad (13)$$

and

$$\tau = \frac{1}{\gamma} \ln\left(1 + \gamma \frac{t}{t_0}\right), \quad (14)$$

with $t_0 = \omega[T(0)]$. Substituting such an expression in (13), we obtain

$$T(t) = \frac{T(0)}{(1 + \gamma t/t_0)^2}, \quad (15)$$

which constitutes the celebrated Haff cooling law. Notice that the cooling law depends on the dimensionality only through t_0 , which represents the free time at the initial temperature $T(0)$. The result has been obtained by neglecting velocity correlations and assuming spatial homogeneity.

Corrections to the constants appearing in Eq. (15) stem from a more careful consideration of the HCS. When the volume fraction is nonnegligible, the Enskog–Boltzmann equation should be employed instead of the Boltzmann equation. This is identical to the Boltzmann equation but for a multiplicative constant in the collision integral that takes into account static density correlations due to the fact that the gas is not perfectly dilute. Very recently it has been shown (Pöschel *et al.*, 2002) that there are also small velocity correlations which must be considered and which modify the molecular chaos hypothesis. With these correlations, the law $T \sim t^{-2}$ is still valid but corrections to the constant γ_0/t_0 appear.

The Haff law can be also derived in the framework of granular hydrodynamics (van Noije *et al.*, 1997; Brey *et al.*, 1998). In the HCS, hydrodynamics can be considered valid as a consequence of homogeneity of the density and velocity field and of the slow

temperature decay. The evolution of the (spatially uniform) temperature field is exactly the same as in Eq. (15).

The velocity distribution functions do not display a Maxwellian shape during the homogeneous cooling regime. The high-velocity tail is overpopulated, whereas the bulk of the distribution is represented by a product of a Maxwellian and a series of Sonine polynomials. Esipov and Pöschel (1997) found that the tail of the velocity distribution function decays as $\exp(-v/v_0)$. We shall see that a slow decay of the velocity distribution is characteristic of systems undergoing inelastic collisions.

It turns out that even in the absence of external fields the HCS is unstable. In fact, when the number of collisions per particle is sufficiently large, one observes a new regime, where the system remains homogeneous in density, but the velocity field develops strong correlations. This is the result of the parallelization of the velocities of the particles induced by inelasticity. A quantitative description of such a phenomenon can be obtained by considering the linear stability of the hydrodynamic modes of the HCS (Brey *et al.*, 1996). Such an analysis shows that a sinusoidal perturbation of the flow field, whose wavelength is long enough, decays slower than the energy mode of the reference homogeneous state. Although this does not mean that the velocity field grows in time, it is an indication that if the velocity field is rescaled by the square root of its variance, then the growth of macroscopic structures (such as vortices) can be observed. Goldhirsch and Zanetti (1993) suggested it as the physical mechanism leading to the formation of high density clusters surrounded by rarefied regions. It was shown that the formation of density clusters appears as a consequence of, and therefore later than, the growth of structures in the velocity field. Therefore there is an intermediate regime between the end of the HCS and the appearance of density clusters. During this regime the velocity field develops spatial structures (and this is put in evidence by a decay of the global kinetic energy which is slower than the Haff t^{-2} decay), while the density remains homogeneous. This consideration allows to study the evolution of velocity spatial structures *keeping homogeneous the density field*, a procedure which we follow in Section 4, where a lattice model with uniform density is investigated.

3. MAXWELL MODELS

The technical difficulties associated with the Boltzmann equation have led to the introduction of a new class of models, the so-called Maxwell models, which lend themselves to a great deal of analytical work (Ernst, 1981). Recently there has been a renewal of interest in these models as a consequence of the introduction of their inelastic variant (Ben-Naim and Krapivsky, 2000) and the discovery of an exact asymptotic scaling solution in 1D (Baldassarri *et al.*, 2002).

There are two equivalent ways of introducing the *elastic* Maxwell models. The first consists in modifying the collision integral in Eq. (3) (with $\alpha = 1$) into a new one:

$$I_M(f, f) = \sigma^{d-1} S(t) \int d\mathbf{v}_2 \int d\hat{\boldsymbol{\sigma}} \{f(\mathbf{v}_1^{**}, t) f(\mathbf{v}_2^{**}, t) - f(\mathbf{v}, t) f(\mathbf{v}_2, t)\}, \quad (16)$$

where $S(t) = \langle (\mathbf{v}_{12} \cdot \hat{\boldsymbol{\sigma}}) \rangle$ is an ensemble average and is proportional to $\sqrt{T(t)}$ (Bobylev, 1975). The prefactor $S(t)$ can be absorbed by a time re-parametrization $t \rightarrow \tau$.

For elastic systems, this is justified by a suitable choice of inter-particle potentials: the so-called Maxwell molecules have a scattering cross-section which is independent from the modulus of the relative velocities, and further approximations on the angular dependence lead to Eq. (16),

Alternatively one can refer directly to an underlying microscopic model which gives rise to the same kinetic equation for the distribution function. Let us consider N particles without positional degrees of freedom and characterized only by their d -dimensional velocities. The dynamics of the system consists of a sequence of events, where pairs of velocities $(\mathbf{v}_i, \mathbf{v}_j)$ are randomly selected and updated according to Eq. (1), with $\alpha = 1$. Since there is no true movement of the grains, the centre to centre direction $\hat{\sigma}$ is randomly chosen with a uniform distribution in the d -dimensional sphere (the “kinematic constraint” can be equivalently disregarded, as it would just randomly avoid half of the collisions to happen). A unit time corresponds to N collisions. This model, for two-dimensional velocities, has been put forward by Ulam (1980). He showed how the velocity distribution asymptotically converges to the Maxwell–Boltzmann distribution, independently from the starting distribution. It leads to the same equation as (16) apart from the prefactor $S(t)$, which can be eventually included by slightly modifying the algorithm described above. The master equation for this stochastic model (including the “kinematic constraint”) can be easily written down:

$$\frac{\partial}{\partial \tau} f(\mathbf{v}, \tau) = \int d\mathbf{v}_2 \int d\hat{\sigma} [f(\mathbf{v}_1^{**}, \tau) f(\mathbf{v}_2^{**}, \tau) - f(\mathbf{v}, \tau) f(\mathbf{v}_2, \tau)] \quad (17)$$

Note that the main physical property that distinguishes the nonlinear Eq. (17) among the family of nonlinear Boltzmann equations (2) is the fact that the collision rate is independent of the energy of the colliding particles. This introduces a dramatic simplification.

It is natural to extend the Maxwell model to the inelastic case, based on the simplest rule (1) with $\alpha < 1$ which ensures momentum conservation during inelastic collisions, by writing

$$I_{\text{IM}}(f, f) = \sigma^{d-1} \int d\mathbf{v}_2 \int d\hat{\sigma} \left\{ \frac{1}{\alpha} f(\mathbf{v}_1^{**}, t) f(\mathbf{v}_2^{**}, t) - f(\mathbf{v}, t) f(\mathbf{v}_2, t) \right\}. \quad (18)$$

The recent surge of interest in this model has been triggered by the discovery of an exact solution (Baldassarri *et al.*, 2001, 2002a,b) for the $d=1$ case with particles having all equal masses. In addition, many properties concerning mixtures with different masses, m_1 and m_2 , and or different coefficients of restitution have been obtained analytically. Extensions to $d > 1$ cases (Ernst, 2002; Ben-Naim and Krapivsky, 2002) have also been analyzed in detail. Let us begin with the simplest case, namely the one-component Maxwell gas with scalar velocities, originally discussed by Ben-Naim and Krapivsky (2000):

$$\frac{\partial f(v, \tau)}{\partial \tau} + f(v, \tau) = \frac{1}{1-\gamma} \int du f(u, \tau) f\left(\frac{v-\gamma u}{1-\gamma}, \tau\right), \quad (19)$$

with $\gamma = (1 - \alpha)/2$.

In order to solve the nonlinear integro-differential Eq. (19) and to be able to treat more complicated models, it is convenient to adopt the Fourier transform method proposed by Bobylev (1975). One employs the characteristic function:

$$\hat{P}(k, \tau) = \int_{-\infty}^{\infty} dv e^{ikv} f(v, \tau), \tag{20}$$

so that Eq. (19) can be rewritten as

$$\partial_{\tau} \hat{P}(k, \tau) = -\hat{P}(k, \tau) + \hat{P}(\gamma k, \tau) \hat{P}((1 - \gamma)k, \tau). \tag{21}$$

Consider the expansion

$$\hat{P}(k, \tau) = \sum_{n=0}^{\infty} \frac{(ik)^n}{n!} \mu_n(\tau). \tag{22}$$

Substituting this expansion into Eq. (21), one obtains an iterative solution, moment by moment. The energy decreases exponentially, since the second moment varies as $v_0^2(\tau) = \int v^2 f(v, \tau) dv = v_0^2(0) \exp[2\gamma(\gamma - 1)\tau]$. Such a power series solution displays an anomaly in the moments, because the rate at which the higher-order moments vanish is lower than that of lower moments. This property seemed to rule out the possibility of a scaling solution, of the form $f(v, \tau) = v_0^{-1} f_s[v/v_0(\tau)]$. However, one can seek the solution under the form of a nonanalytic expansion for small values of k under the form

$$\hat{P}(k v_0) = 1 - k^2 v_0^2 + A(k v_0)^{\sigma} + \text{higher-order terms},$$

and obtain the following transcendental equation for the indicial exponent σ :

$$\sigma = \frac{\gamma^{\sigma} + (1 - \gamma)^{\sigma} - 1}{\gamma(1 - \gamma)},$$

which has a solution for $\sigma = 3$, independent from γ . The presence of such a singularity in the small- k expansion implies a slow asymptotic decay of the distribution function $f(v, \tau) \propto v^{-\sigma-1}$ for large values of the argument.

In Baldassarri *et al.* (2002a), the complete form of such a distribution was discovered, which reads

$$\hat{P}(k v_0) = (1 + |k| v_0) \exp(-|k| v_0), \tag{23}$$

and shows the presence of diverging moments of order $n \geq 4$ and of the predicted nonanalyticity $|k|k^2$ near the origin. Going back to the original velocity representation, one finds:

$$f(v, \tau) = \frac{2}{\pi v_0(\tau) \{1 + [v/v_0(\tau)]^2\}^2}, \tag{24}$$

which is indeed a solution of the nonlinear Boltzmann Eq. (19). It is remarkable that the form of such a solution is independent of the coefficient of restitution, α (Baldassarri *et al.*, 2001, 2002a,b), which only determines the rate at which the energy is dissipated.

3.1. Higher Dimensions

For higher dimensions, the problem of a scaling solution has been recently addressed in (Ernst and Briton, 2002; Nie *et al.*, 2002). The numerical indication shown in Fig. 1 of large algebraic tails for models with $d > 1$ has been recently confirmed by several analytical studies (Ben-Naim and Krapivsky, 2002; Ernst and Brito, 2002). These works compute self-consistently the exponents for arbitrary dimension considering the first singular term in the $x \rightarrow 0$ behaviour for the Fourier-transformed scaling function $\hat{P}(\mathbf{x})$, with $x = kv_0$. First consider the isotropic solution

$$\hat{P}(\mathbf{x}) = \psi(x^2).$$

If the corresponding scaling solution has algebraic tails for large y of the form

$$f(\mathbf{y}) \propto y^{-2a-d},$$

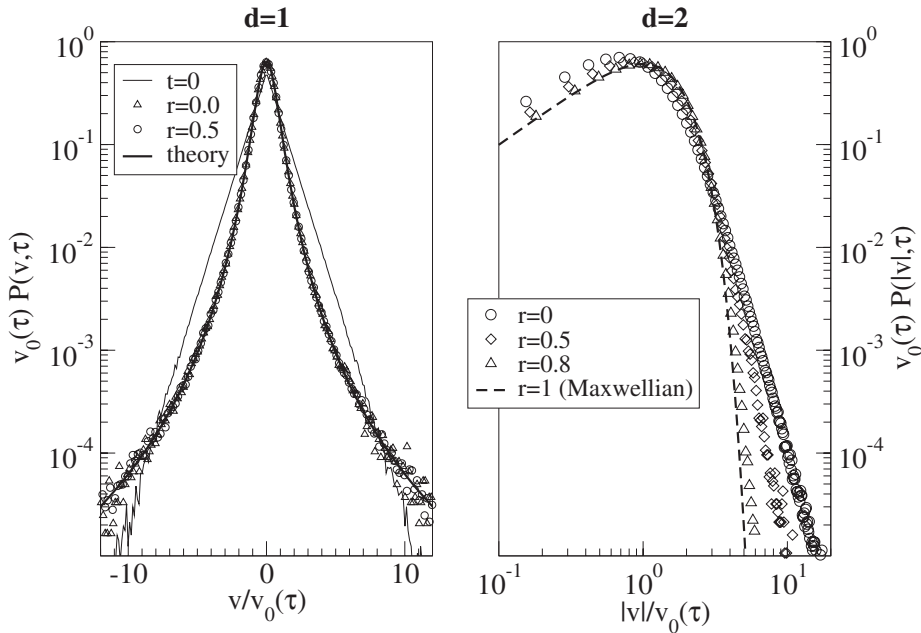


FIGURE 1 Asymptotic velocity distributions $P(v, \tau)$ vs. $v/v_0(\tau)$ for different values of restitution coefficient ($\alpha \equiv r$) from the simulation of the inelastic Maxwell model in one dimensions (left) and two dimensions (right). In one dimensions the asymptotic distribution is independent of α and collapses to Eq. (24). In one dimensions, the chosen initial distribution (exponential) is drawn (same result with uniform and Gaussian initial distribution). In two dimensions the distributions still present power-law tails, but the power depends on α : for $\alpha \rightarrow 1$ the p.d.f. tends to a Maxwell distribution. Data refer to more than $N = 10^6$ particles.

then its Fourier transform for small values of the argument is

$$\psi(z) \simeq 1 + \frac{1}{2}z + \sum_{m < a} \frac{\mu_{2m}}{(2m)!} z^m + Az^a + O(z^a). \quad (25)$$

Inserting the form (25) in the Fourier-transformed equation for the isotropic scaling solution and equating the coefficients of equal powers of z an equation for a can be obtained. We refer to (Ben-Naim and Krapivsky, 2002; Ernst and Brito, 2002) for the detailed derivation of the final transcendental equation:

$$1 - \lambda \left(a - \frac{d}{2} \right) = \int_0^1 \mathcal{D}\mu [\xi^{a-d/2} + \eta^{a-d/2}], \quad (26)$$

where

$$\mathcal{D}\mu = \frac{\mu^{-1/2}(1-\mu)^{(d-2)/2}}{B(1/2, (d-1)/2)} d\mu, \quad (27a)$$

$$\xi = 1 - [3 + \alpha(2 - \alpha)] \frac{\mu}{4}, \quad (27b)$$

$$\eta = (1 + \alpha) \frac{\mu}{4}, \quad (27c)$$

and $\lambda = (1 - \alpha^2)/d$, while $B(x, y)$ is the beta function which guarantees the proper normalization $\int_0^1 \mathcal{D}\mu = 1$. Equation (26) (which can be solved numerically) gives the exponent a for a generic dimension $d > 1$ and restitution coefficient α . In the elastic limit $\alpha \rightarrow 1$ the exponent $a \rightarrow \infty$, indicating that one recovers the Gaussian Boltzmann distribution tail. Results of our numerical simulations for the two-dimensional case are shown in the right frame of Fig. 1. For $\alpha = 1$ we recover the asymptotic Maxwell distribution predicted by Ulam, whereas for $\alpha = 0$ our data suggest the formation of algebraic tails.

3.2. The Inelastic Maxwell Mixture

Interesting features also emerge when the inelastic Maxwell model is extended to treat grains having different physical properties, such as unequal masses, different coefficients of restitution, different radii, etc. The binary Maxwell mixture with scalar velocities was considered in (Marini Bettolo Marconi and Puglisi, 2002a,b). The system consists of N_1 particles of species 1 and N_2 particles of species 2 endowed with scalar velocities v_i^α , with $\alpha = 1, 2$ and $i = 1, N_\alpha$. The two species may have different masses, m_1 and m_2 and/or different restitution coefficients $\alpha_{11}, \alpha_{22}, \alpha_{12} = \alpha_{21}$. The collision rule is modified in the following way:

$$v_i^\alpha = v_i^\alpha - (1 + \alpha_{\alpha\beta}) \frac{m_\beta}{m_\alpha + m_\beta} (v_i^\alpha - v_j^\beta), \quad (28a)$$

$$v_j^\beta = v_j^\beta + (1 + \alpha_{\alpha\beta}) \frac{m_\alpha}{m_\alpha + m_\beta} (v_i^\alpha - v_j^\beta). \quad (28b)$$

In order to construct the solution, one considers the Fourier transform of the velocity distribution functions for the two components:

$$\begin{aligned} \partial_t \hat{P}_1(k, t) = & -\hat{P}_1(k, t) + p \hat{P}_1(\gamma_{11}k, t) \hat{P}_1((1 - \gamma_{11})k, t) \\ & + (1 - p) \hat{P}_1(\tilde{\gamma}_{12}k, t) \hat{P}_2((1 - \tilde{\gamma}_{12})k, t), \end{aligned} \tag{29a}$$

$$\begin{aligned} \partial_t \hat{P}_2(k, t) = & -\hat{P}_2(k, t) + (1 - p) \hat{P}_2(\gamma_{22}k, t) \hat{P}_2((1 - \gamma_{22})k, t) \\ & + p \hat{P}_2(\tilde{\gamma}_{21}k, t) \hat{P}_1((1 - \tilde{\gamma}_{21})k, t), \end{aligned} \tag{29b}$$

where $p = N_1/(N_1 + N_2)$, $\zeta = m_1/m_2$, and

$$\gamma_{\alpha\beta} = \frac{1 - \alpha_{\alpha\beta}}{2}, \tag{30a}$$

$$\tilde{\gamma}_{12} = \left[1 - \frac{2}{1 + \zeta} (1 - \gamma_{12}) \right], \tag{30b}$$

$$\tilde{\gamma}_{21} = \left[1 - \frac{2}{1 + \zeta^{-1}} (1 - \gamma_{12}) \right]. \tag{30c}$$

By expanding the characteristic functions \hat{P}_α in powers of k one finds expressions for the higher moments of the velocity distributions in terms of lower moments. In particular, one observes that the average kinetic energies of the two components are different, but asymptotically decrease at the same rate, i.e., there is no energy equipartition. In other words, their ratio reaches asymptotically a constant value, $T_1/T_2 \neq 1$ (see Fig. 2). Such a feature agrees with the result obtained in the framework of the Boltzmann–Enskog transport equation by Garzò and Dufty (1999) for the IHS.

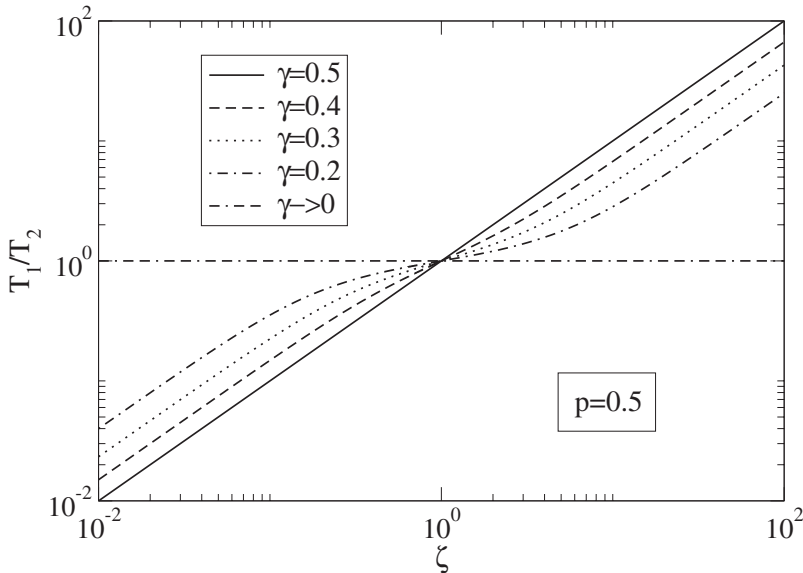


FIGURE 2 Ratio $T_1(\infty)/T_2(\infty)$ between asymptotic temperatures of the two components of the mixture, as a function of the mass ratio ζ , for different values of the inelasticity parameter $\gamma_{11} = \gamma_{22} = \gamma_{12} = \gamma = (1 - \alpha)/2$, where α is the restitution coefficient. $p = 0.5$ for all the curves. The perfectly elastic case is the horizontal line, which represents energy equipartition.

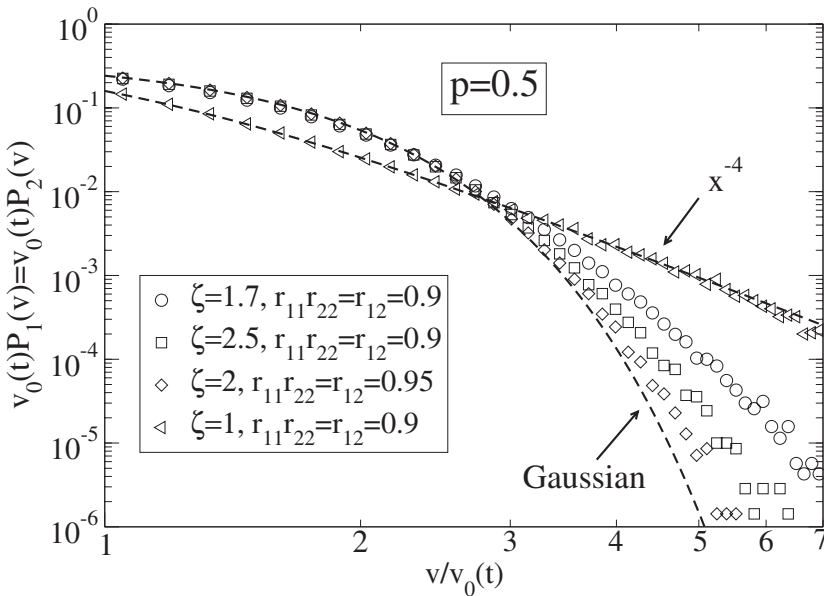


FIGURE 3 Tails of the rescaled asymptotic velocity distributions from numerical simulations of the model with number ratio $p = 0.5$ and different values of the restitution coefficients and of the mass ratio ζ . The pure case $\zeta = 1$ has the exact asymptotic solution $P(x) = (2/\pi)(1 + x^2)^{-2} \sim x^{-4}$. The Gaussian is shown as a guide for the eye.

The scaling solution for the inelastic mixture, can be obtained by extending the method proposed by Ernst and Brito (2002) of the previous section, which gives a transcendental equation for the indicial exponent, σ , characterizing the singularity. One finds that the velocity distributions associated with the two components in general differ in shape and possess power law tails (see Fig. 3). Remarkably, the exponent associated with these tails takes on values between 2 and ∞ , depending upon the parameters of the system. In other words, it means that the inverse-power law tails of the distribution are sensitive to the composition, to the mass ratio and to the nature of the interactions in the mixture. The value of the exponent does not depend on a simple way on the control parameters. The value $\sigma = 3$ of the pure system represents only a special case. In fact, the larger the mass ratio the larger the deviation from $\sigma = 3$ (see Fig. 4).

4. MODELS WITH SPATIAL STRUCTURE

A large number of studies has been devoted to the dynamics of freely cooling granular gases in various dimensions $1 \leq d \leq 3$. In realistic models, such as the IHS model, as mentioned above, inelastic collisions generate spatial correlations and determine the formation of structures. The difficulties associated with the presence of strong spatial gradients and nonlinearities, however, render extremely difficult a proper theoretical understanding of the late stages of the cooling process. On one hand, due to the neglect of velocity correlations, the Enskog–Boltzmann equation is not suitable for investigating such a regime. On the other hand, inelastic Maxwell models, in view of

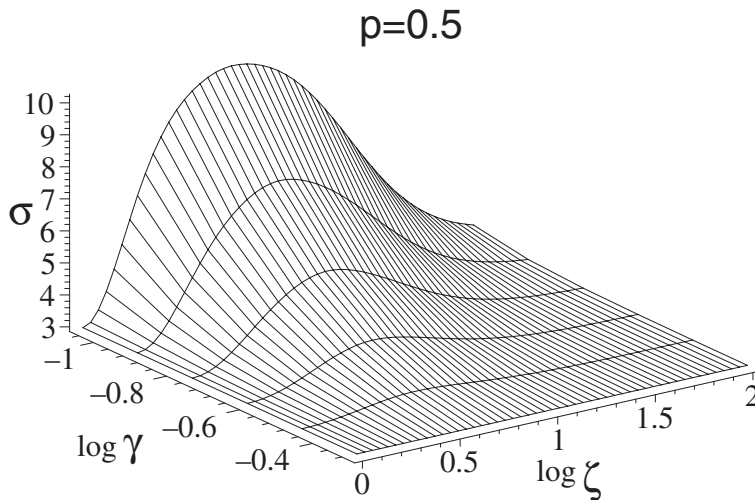


FIGURE 4 Power of the singularity σ of the solution of the coupled master equations for the mixture model, as a function of the mass ratio ζ and the inelasticity parameter $\gamma_{11} = \gamma_{22} = \gamma_{12} = \gamma = (1 - \alpha)/2$. Here α is the restitution coefficient, and $p = 0.5$.

the mean-field coupling by which each molecule may interact with all the remaining molecules regardless of their relative position, are not able to reproduce any spatial ordering. However, one can preserve the relative simplicity of the Maxwell models and introduce a spatial structure by assigning N velocities to the N nodes of a regular lattice. The initial velocities are chosen randomly from a Gaussian distribution. The velocity of a particle changes only when it participates to a collision with one of its lattice nearest neighbours, according to the rule in Eq. (1). The updating is performed by a random selection of the colliding pairs and occurs only when the projection of the relative velocity along the direction connecting the particles is negative. Other variants of the model do not include such a kinematic constraint. Notice also that the velocity of the i th particle is not the time derivative of its position and the particle density is not a dynamical variable of the model and that the choice of colliding particles does not depend on the modulus of the relative velocity. This is why we consider this an “inelastic Maxwell model” embedded in a lattice. In this model the only measure of time is τ , i.e., the cumulated number of collisions per particle. Recently the one-dimensional case of this model has been studied (Ostojic *et al.*, 2004), showing further remarkable connections with the one-dimensional gas of inelastic particles.

4.1. The One-dimensional Lattice

First we consider the case of a linear lattice and of scalar velocities. In order to define the model, let us assign N scalar velocities to the N nodes of a line and assume periodic boundary conditions. The process consists of collisions between two neighbouring nodes. Every colliding pair is chosen randomly with uniform probability, considering only pairs with $v_i - v_{i-1} < 0$, i.e., pairs that can physically collide (this is what we call the “kinematic constraint”). The collision rule is given, as usual, by Eq. (1). A

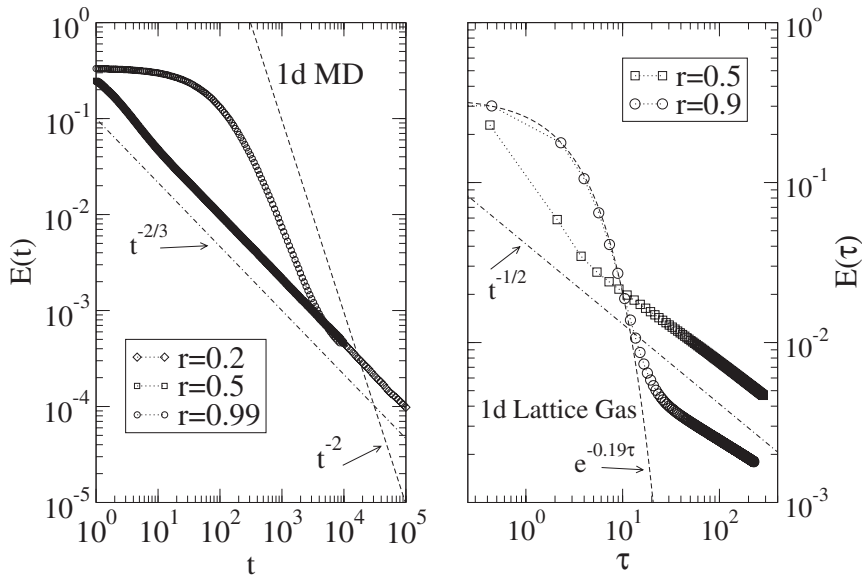


FIGURE 5 Time-dependence of kinetic energy for the inelastic hard rods (left) and for the inelastic lattice Maxwell model (right). The homogeneous Haff stage is evident only for quasi-elastic systems, whereas the more inelastic systems enter almost immediately into the correlated regime. Note the different time units used (t is the physical time, defined only in MD simulations, while τ is the cumulated number of collisions per particle). The Haff law $E \sim t^{-2} \sim \exp(-\gamma_0 \tau)$ is verified for both systems. The correlated regime presents a behaviour $t^{-2/3}$ independent of α for the hard rods, while appears diffusive (in collision units) $\tau^{-1/2}$ and α -dependent for the lattice model. Data refer to $N = 10^6$ particles (both models).

unit of time corresponds to N collisions: time is indicated with the symbol τ in order to recall that it is just a measure of the number of collisions in this process and *cannot* directly be compared with time of simulations of realistic models. To show the similarities between the dynamics of this lattice model and that of a simulation of N inelastic hard rods moving on a line, we show the results of both systems.

The time-evolution of the kinetic energy per particle $E = (1/N) \sum v_i^2$ is displayed in Fig. 5. The lattice model (right frame) reproduces the Haff regime $E(\tau) \sim \exp(-\gamma_0 \tau)$, and successively displays a decay of the form $\sim \tau^{-1/2}$. The homogeneous Haff stage is evident only in the case of quasi-elastic systems, whereas, in the more inelastic cases one observes almost immediately the second regime. The $\exp(-\gamma_0 \tau)$ decay of the energy is expected during the initial stage of the evolution of the lattice system as a consequence of the lack of correlation between colliding pairs. When the energy decay departs from the Haff law, it is a signature of the emergence of correlations between velocities. The hard rods system (left frame) presents again the Haff regime (which, in the physical time, appears as $E \sim t^{-2}$), and successively an energy decay of the kind $E \sim t^{-2/3}$. This second stage is again a consequence of velocity correlations. It is not possible to make a strict comparison between the energy decay of the lattice system with that of the hard rods system because the collision rate in the lattice model is 1 even in the correlated phase, while in the hard rods model it changes with time. Moreover, the simulation of the hard rods model is performed using a particular “regularization” that avoids inelastic collapse (Ben-Naim *et al.*, 1999). A very small cut-off velocity is chosen and, whenever the relative velocities of two colliding particles are lower than this cut-off the collision happens with $\alpha = 1$, i.e., elastically. If the value

of the cut-off is changed but remains much lower than the square root of the minimum energy E observed, the evolution of $E(t)$ does not change at all, but the evolution of the collision rate changes. Therefore the collision rate depends upon the “regularization” while the energy does not depend on it, and this makes a nontrivial mapping between the time t , used in the hard rods simulations, and the time τ used in the lattice model. We will show that a good comparison can be obtained for other observables, using the energy E itself as a clock. Another difference between the hard rods model and the lattice one is the dependence on the restitution coefficient. The asymptotic decay of the energy for the hard rods *does not* depend upon α , while depends upon it for the velocities on the lattice.

The analysis of the probability density function (p.d.f.) of the velocities, $P(v, t)$, presented in Fig. 6, is another indication that the lattice models have strong similarities with the hard rods model, and also that in the second stage of the energy decay there are strong correlations between velocities. In fact the homogeneous, uncorrelated, version of the lattice model is the inelastic Maxwell model considered in the previous section, for which a p.d.f. with power law tails is expected. On the contrary, the velocity p.d.f. of the lattice model (which is obtained by simply applying the inelastic Maxwell model on a two-neighbour topology) is identical to the velocity p.d.f. with two peaks observed in the Haff regime of the hard rods system. This p.d.f. is compatible with the solution of the Boltzmann equation for inelastic hard rods, which is a sum of two delta functions (Benedetto *et al.*, 1997).

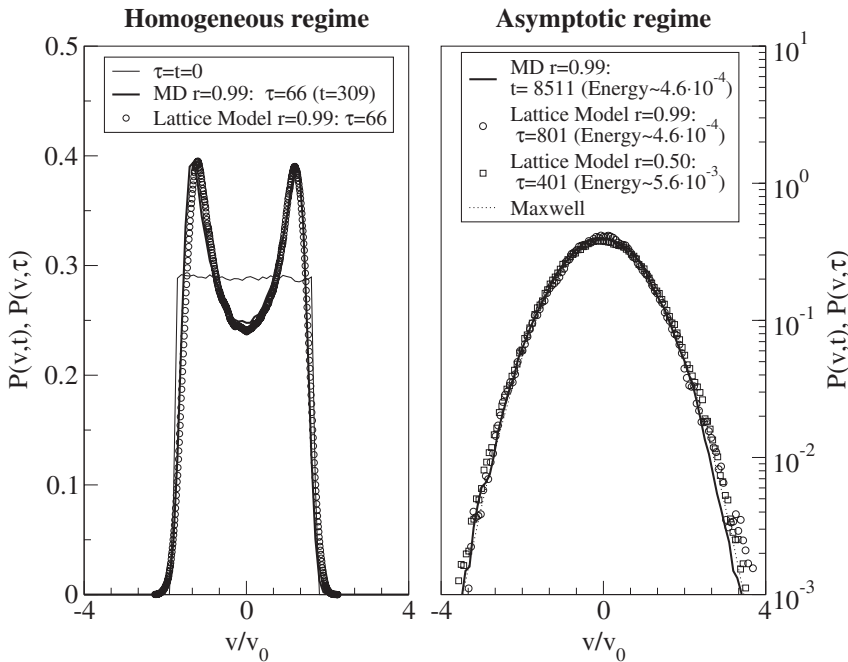


FIGURE 6 Rescaled velocity distributions for the hard rods system and the one-dimensional inelastic Maxwell model, during the homogeneous (left) and the inhomogeneous phase (right). In the left frame there is also shown the initial distribution (both models). The distributions refer to systems having the same energy. Data refer to $N = 10^6$ particles (both models) with $\alpha = 0.99$ and 0.5 (for the lattice model in the inhomogeneous regime).

The observation of global quantities such as the energy or the velocity p.d.f. indicates that the lattice model possesses an initial uncorrelated regime followed by a second correlated regime. It is therefore interesting to characterize the spatial structures of the velocity field, starting with the analysis of the velocity profile. The comparison of the velocity profiles of the lattice model with those observed in the hard rods system must be carefully carried out whereas in the lattice model the particles cannot move. As a consequence of this fact we find that a better comparison between the two models is obtained when the profile v_i of the hard rods system is plotted *versus* the particle index i instead of its position x_i . Shocks are typical defects in the correlated regime of the hard rods model as they appear as descending jumps of the velocity profile followed by slow ascending slopes. Particles to the left and right of a shock continue to collide, entering the shock, while particles in the slow slopes do not collide and flow toward other shocks. In correspondence of shocks there are high density clusters of particles. Eventually the dynamics leads to only one cluster. Such a scenario is evident in the top frame of Fig. 7. The good agreement between hard rods and the inelastic Maxwell model on the lattice can be appreciated in the two bottom panels of the same figure. Using as abscissa i instead of x_i , the shocks observed in the simulations of hard rods appear reversed and smoothed, making the v -profile very similar to the one observed in the lattice model. In Ostojic *et al.*, this comparison has been carried on systematically. The authors have observed that the hard rods system, from the point of view of the velocity profile, is equivalent to a lattice model with a peculiar choice of the sequence of colliding pairs (the order is given by relative velocities and

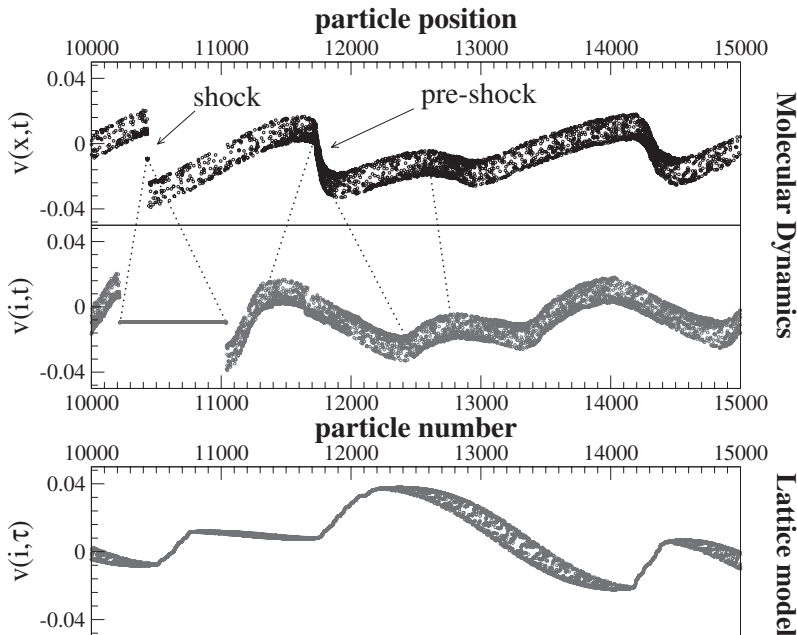


FIGURE 7 Portions of the instantaneous velocity profiles for the hard rods (top $v(x, t)$, middle $v(i, t)$) and for the one-dimensional lattice model (bottom, $v(i, \tau)$). In the middle frame we display the profile of the hard rods system against the particle label in order to compare the shocks and preshocks structures with the lattice model (the dotted lines show how shocks and preshocks transform in the two representations for the hard rods). Data refers to $N = 2 \times 10^4$ particles, $\alpha = 0.99$ (both models).

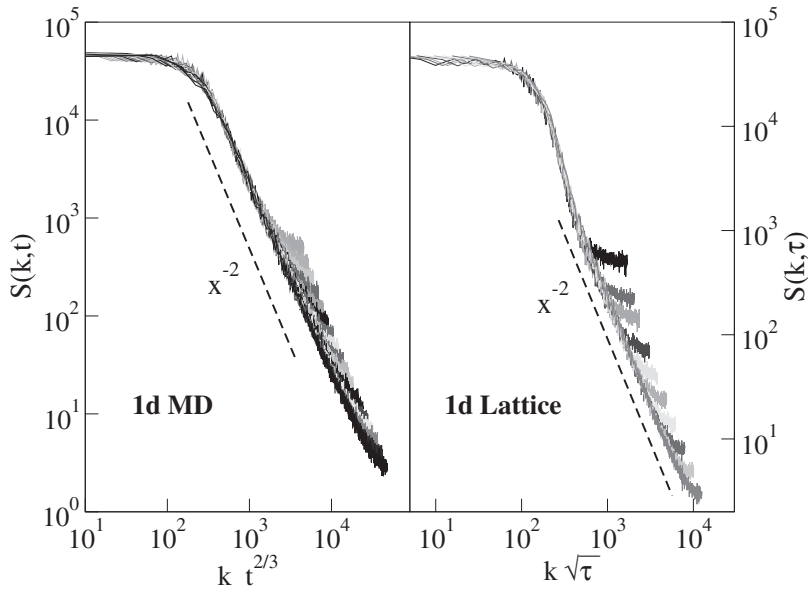


FIGURE 8 Structure factors $S(k, t)$ against $kt^{2/3}$ for the one-dimensional MD and against $k\tau^{1/2}$ for the one-dimensional lattice gas model, in the inhomogeneous phase. Times are chosen so that the two systems have the same energies. Data refers to system with more than $N = 10^5$ particles, $\alpha = 0.5$ (both models).

positions), and also that the dynamics on the lattice depends weakly upon the choice of the order of colliding particles. This observations lead to the consideration that the hard rods model and the inelastic lattice Maxwell model are in a sort of common class of universality together with the gas of sticky particles, whose velocity profile is governed by the Burgers equation (this has been also conjectured in (Ben-Naim *et al.*, 1999).

A better characterization of the structures that appear in the velocity field after the Haff regime can be achieved by considering the velocity structure function, shown in Fig. 8. In the lattice model we obtain a good collapse of structure factors calculated at different times τ if we plot $S(k)$ against $k\tau^{1/2} \sim 1/E(\tau)$. This indicates that the correlation length grows diffusively, i.e., $L \sim \tau^{1/2}$ with L the typical size of structures in the velocity field. The $S(k)$ presents two main features: a large-scale Gaussian-like behaviour (expected for a diffusive dynamics), and a k^{-2} behaviour at high values of k (short-scales) which is a signature of topological defects. The structure function for the hard rods system, calculated for the velocity field v_i as a function of i , is identical to that coming from the lattice model. In this case the collapse is obtained using $kt^{2/3} \sim 1/E(t)$ as abscissa, revealing that a general “clock” for the growth of correlations, valid in both models, is the energy E . Finally, we stress the relevance of the kinematic constraint. If one removes it, the resulting dynamics becomes equivalent to a diffusive process for the velocity field, whereas the defects disappear.

4.2. The Two-dimensional Lattice

Here we present some aspects of the two-dimensional lattice model, with particular emphasis to its spatial structure, determined by a new kind of topological defects, namely vortices, not present in one dimension. The off-lattice counterpart of the

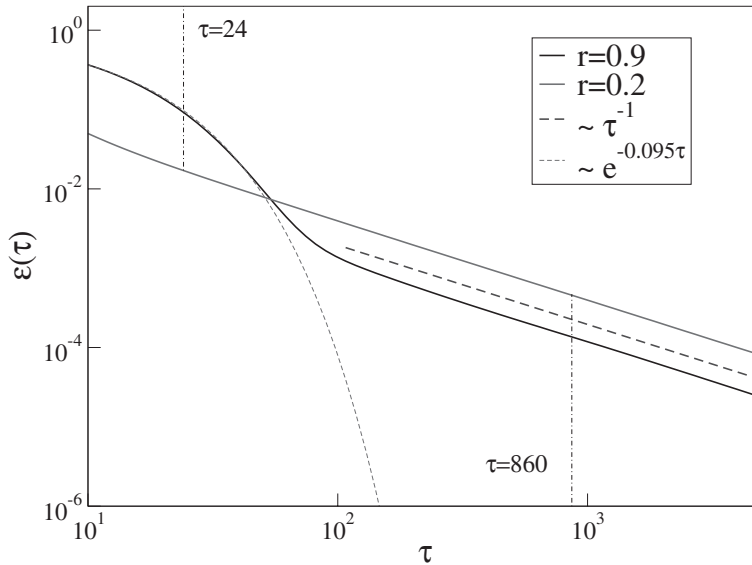


FIGURE 9 Energy decay for the 2d lattice model with $\alpha = 0.9$ and 0.2 (1024^2 sites). The bold dashed line $\sim 1/\tau$ is a guide to the eye for the asymptotic energy decay, while the light dashed line is the exponential fit corresponding to the Haff law $\exp(-2\gamma_0\tau)$. The Haff regime is too short to be observed in the system with $\alpha = 0.2$. The two indicated times $\tau=24$ and 860 correspond to the plots of Fig. 15.

model is the gas of inelastic hard disks. In two dimensions the particles are characterized by a 2-component vector velocity \mathbf{v}_i and are placed on a triangular lattice with positions \mathbf{r}_i . The velocities are updated in a random sequence and the kinematic constraint requires $(\mathbf{v}_i - \mathbf{v}_j) \cdot (\mathbf{r}_i - \mathbf{r}_j) < 0$.

We first inspect the decay of the energy (Fig. 9), which shows again the presence of two distinct regimes. The first exponential decay, representing the Haff regime, is the result of the fact that during the initial evolution of the system the velocities remain independent. Only when the statistical independence between velocities is reduced and spatial correlations develop, the energy evolution becomes slower and follows a τ^{-1} decay. The power law decay in the correlated regime is compatible with that observed in the 1d model, and a general formula for any dimensionality $E \sim \tau^{-d/2}$, in agreement with the conjecture of a diffusive behaviour, can be extrapolated.

The rescaled velocity p.d.f.'s (see Fig. 10) are non-Gaussian in the homogeneous (uncorrelated) regime: in such a regime the Boltzmann equation for hard disks predicts exponential tails (Esipov and Pöschel, 1997) for the velocity p.d.f. and this prediction seems adequate also for the lattice model. In the second stage of the energy decay, when the Haff law ceases to hold, the velocity distribution appears more similar to a Gaussian. Such a “return-to-the-Gaussian” phenomenon has been already observed in inelastic hard disks simulations (Huthmann *et al.*, 2000; Nakanishi, 2002; Nie *et al.*, 2002; Das and Puri, 2003). In this stage, however, the velocity field is far from being homogeneous (as we show in the following), so that the Gaussian behaviour of the global velocity p.d.f. could simply be the signature of the presence of many independent domains.

In correspondence of the crossover from the Haff energy decay to the $1/\tau$ decay, one can observe a dramatic change in the properties of the velocity field. The inelasticity has

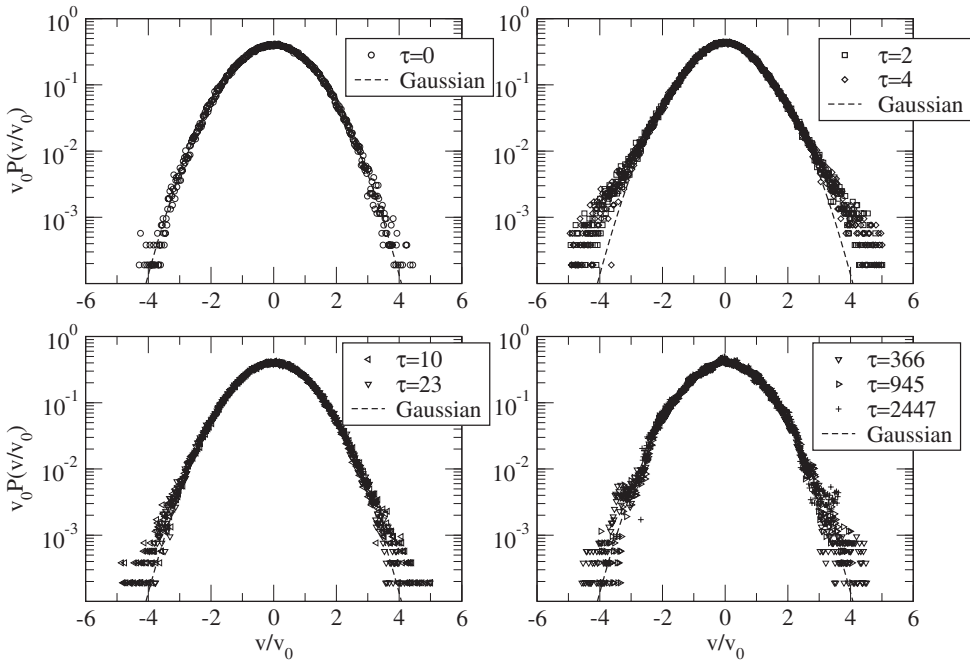


FIGURE 10 Distributions of horizontal velocity at different times for the same system, a 2d lattice Maxwell model with $\alpha = 0.2$ and $N = 512 \times 512$. The distributions are rescaled in order to have unit variance. The initial distribution is a Gaussian. The distribution becomes broader in the uncorrelated phase (first regime), and then turns back toward a Gaussian.

the effect of inducing an alignment of the velocities of neighbouring spins. At the same time the conservation of momentum prevents a global alignment of all the vectors of the velocities. The best alignment that can be obtained with the constraint of momentum conservation is the formation of vortices and in fact they can be easily observed in this regime, see Fig. 11. The presence of the “kinematic constraint” also induces shock-like structures. The characterization of spatial structures is achieved by means of the equal-time structure functions

$$S^{t,l}(k, \tau) = \sum_{\hat{k}} \mathbf{v}^{t,l}(\mathbf{k}, \tau) \mathbf{v}^{t,l}(-\mathbf{k}, \tau), \quad (31)$$

where the superscripts t, l indicate the transverse and longitudinal components of the field with respect to the wave vector \mathbf{k} and the sum $\sum_{\hat{k}}$ is over a circular shell of radius k . The collapse shown in Fig. 12, obtained by plotting several structure functions measured at different instants against the rescaled wavevector $k\tau^{1/2}$ indicates the presence of dynamical scaling. The small-wavevector portion of the structure functions, associated with the growing size of the vortices $L(\tau) \sim \tau^{1/2}$, has a Gaussian shape analogous to the one observed in the domain growth problem. The large-wavevector structure, which is more evident for larger values of α , reflects the internal noise, that is the short-range disorder induced by the collisions. The less elastic system does not present such a plateau, but a decay k^{-4} at small scales which is analogous to the Porod law (Porod, 1951) is expected from the presence of defects in a phase ordering process.

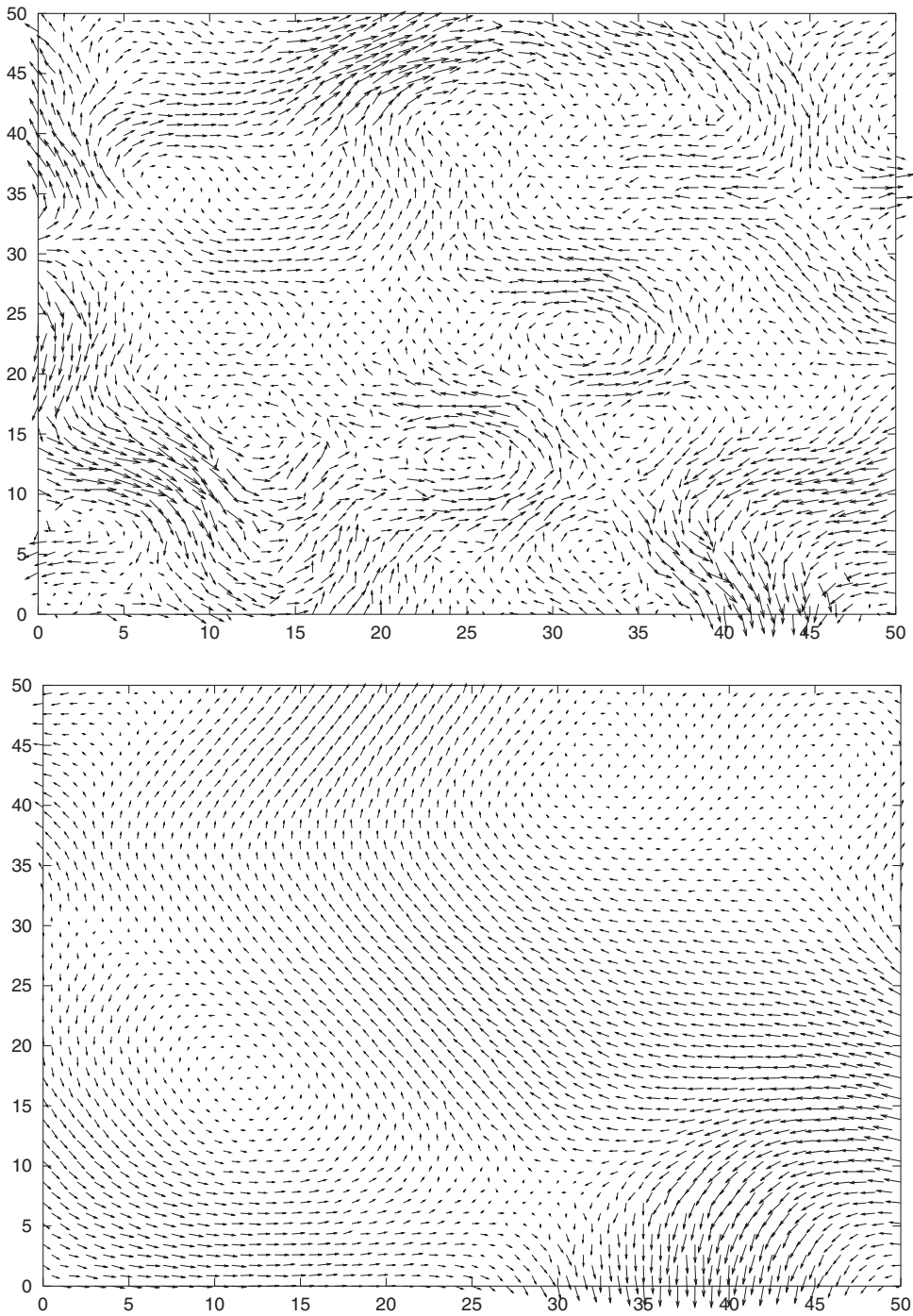


FIGURE 11 A (zoomed) snapshot of the velocity field in the two-dimensional lattice at time $\tau = 52$ (top), with $\alpha = 0.7$ and size $N = 512 \times 512$. The time has been chosen at the beginning of the correlated regime. It is evident in the presence of vortices. All the velocities have been rescaled to arbitrary units, in order to be visible. Another snapshot of the same system at a later time $\tau = 535$ (bottom). The diameter of the vortices has grown. All the velocities have been rescaled to arbitrary units, in order to be visible.

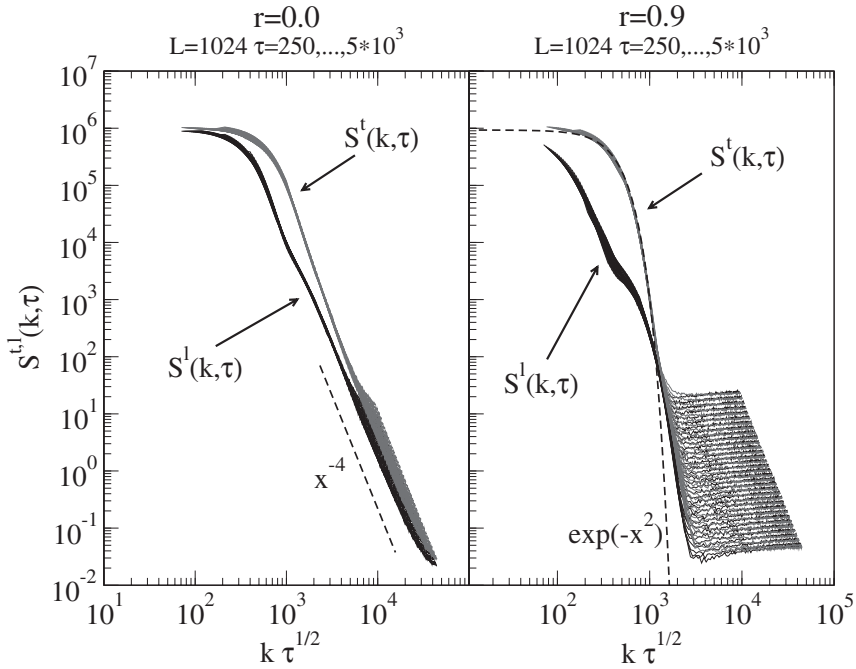


FIGURE 12 Data collapse of the transverse (S^t) and longitudinal (S^l) structure functions for $\alpha=0$ and 0.9 (system size 1024^2 sites, times ranging from $\tau=500$ to 10^4). The wave number k has been multiplied by $\sqrt{\tau}$. Notice the presence of the plateaus for the more elastic system. For comparison we have drawn the laws x^{-4} and $\exp(-x^2)$.

4.2.1. Shocks

Shocks in the velocity field are revealed by the distribution of longitudinal and transversal velocity differences, defined as

$$U_l(\mathbf{R}) = (\mathbf{v}_{i+\mathbf{R}} - \mathbf{v}_i) \cdot \frac{\mathbf{R}}{R}, \quad (32a)$$

$$U_t(\mathbf{R}) = (\mathbf{v}_{i+\mathbf{R}} - \mathbf{v}_i) \times \frac{\mathbf{R}}{R}, \quad (32b)$$

and whose analysis is shown in Fig. 13. The main graph contains the case $R=1$, i.e., the distributions of velocity gradients. Both the longitudinal and transversal components are distributed with non-Gaussian tails, but the longitudinal component presents also a strong asymmetry. This reveals that there are strong velocity differences in the direction of growing longitudinal velocity which are not counterbalanced by similar differences in the opposite direction. Such an asymmetry recalls the “shocks” of the 1d lattice model (the bottom panels of Fig. 7). On the contrary, when $R \gg 1$, the distribution of velocity differences is a Gaussian.

To summarize, vortices determine the algebraic decay of the velocity structure functions, whereas shocks are responsible for the non-Gaussian shape of the probability densities of longitudinal and transversal velocity increments. Instead, the plateau in the tail of the structure functions is related to the internal noise mechanism, i.e., to

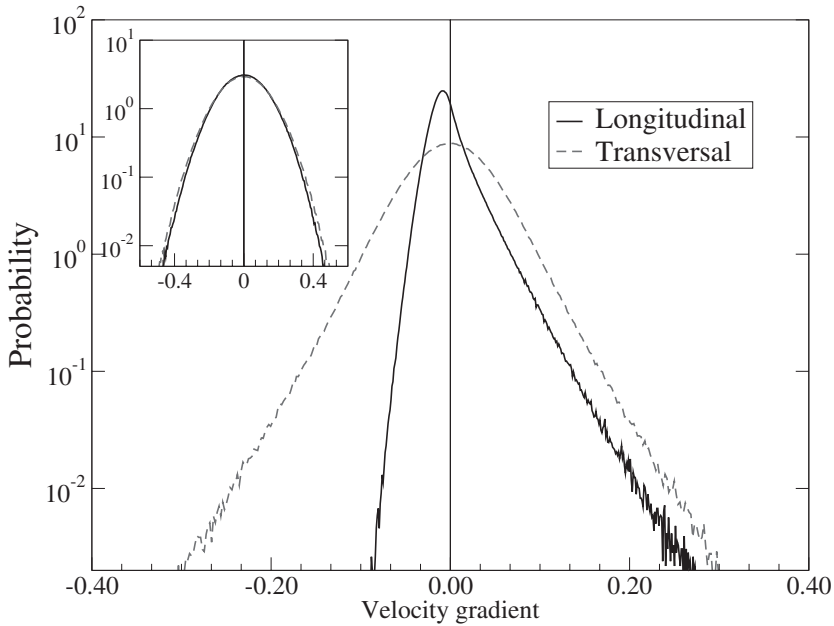


FIGURE 13 Probability densities of the longitudinal and transverse velocity increments. The main figure shows the p.d.f. of the velocity differences for $R=1$. The inset shows the Gaussian shape measured for $R=40$ (larger than $L(t)$ for this simulation: $\alpha=0.2$, $t=620$, system size 2048^2).

the presence of short-range spatial fluctuations induced by the random collisions. A small coefficient of restitution determines a rapid locking of the velocities of neighbouring “spins” to a common value, whereas for $\alpha \rightarrow 1$, short-range small-amplitude disorder persists within the domains, determining an appreciable deviation from the scaling of $S^{t,l}$ for large wavevectors.

4.2.2. Autocorrelations

To complete the analysis of the dynamics of the system we have considered the behaviour of the two-time self-correlation of the velocity components:

$$C(\tau_1, \tau_2) = \frac{1}{N} \sum_i v_i(\tau_1) v_i(\tau_2). \quad (33)$$

There is a short-time transient during which the self-correlation is time translational invariant (TTI), i.e., it depends only on $\tau_1 - \tau_2$. Later, $C(\tau_1, \tau_2)$ depends just on the ratio $x = \tau_1/\tau_2$, which is a feature of “aging” systems. The presence of such two regimes is similar to what occurs during the coarsening process of a quenched magnetic system. After a time τ_w from the quench, the self-correlation of the local magnetization $a(\tau_w, \tau_w + \tau)$ for $\tau \ll \tau_w$ shows a TTI decay toward a constant value $m_{\text{eq}}^2(T_{\text{quench}})$ that is the square of the equilibrium magnetization. This means that the local magnetization is evolving in an ergodic-like fashion. Successively the self-correlation decays with the *aging* scaling law indicated above. In our model the behaviour of the self-correlation

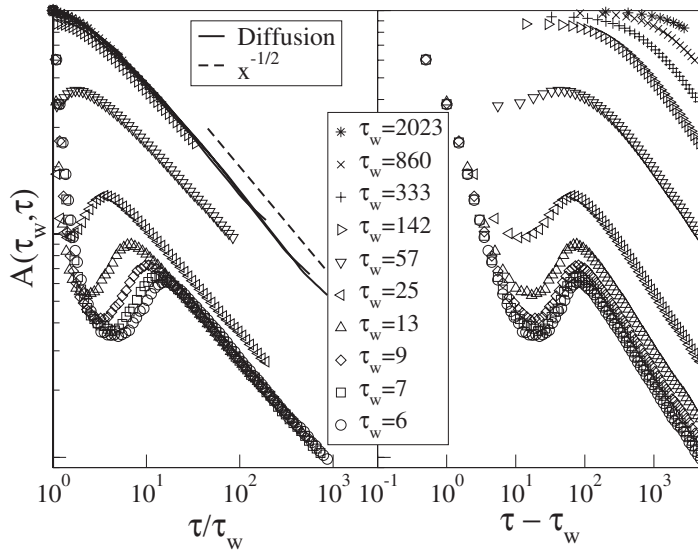


FIGURE 14 Angular autocorrelation function $A(\tau, \tau_w)$ in the two-dimensional lattice model for different values of the waiting time τ_w , and $\alpha = 0.9$ (1024^2 sites). The graph on the left shows the convergence to the τ/τ_w diffusive scaling regime, for large τ_w . For small τ_w , a local minimum is visible (for such a quasi-elastic dynamics). In the graph on the right the same data are plotted vs. $\tau - \tau_w$: note that the small τ_w curves tend to collapse. For higher τ_w the position of the local minimum does not move sensibly, but its value grows and goes to 1 for large τ_w .

is even more subtle, as the cooling process imposes a (slowly) decreasing “equilibrium” temperature $T_{\text{quench}} \rightarrow 0$. This progressively erodes the TTI regime and better resembles a finite rate quench. The same dependence on the TTI manifests itself in the angular autocorrelation, shown in Fig. 14:

$$A(\tau, \tau_w) = \frac{1}{N} \sum_i \cos[\theta_i(\tau_w + \tau) - \theta_i(\tau_w)]. \tag{34}$$

The nonmonotonic behavior of $A(t, t_w)$ suggests that the initial direction of the velocity induces a change in the velocities of the surrounding particles, which in turn generates, through a sequence of correlated collisions, a kind of retarded field oriented as the initial velocity. As t_w increases the maximum is less and less pronounced.

4.2.3. Hydrodynamic Scale

An open issue in the study of granular gases is the possibility of giving a hydrodynamics description of their dynamics. The usual kinetic theory procedures (for example the Chapman–Enskog expansion) require that there is a mesoscopic scale which separate the fast modes, which decay rapidly in space and time, and the slow modes which can be described by hydrodynamics equations. The existence of slow modes is usually guaranteed by conservation laws, but the absence of energy conservation poses doubts about the validity of scale separation for the temperature field. In the lattice model that

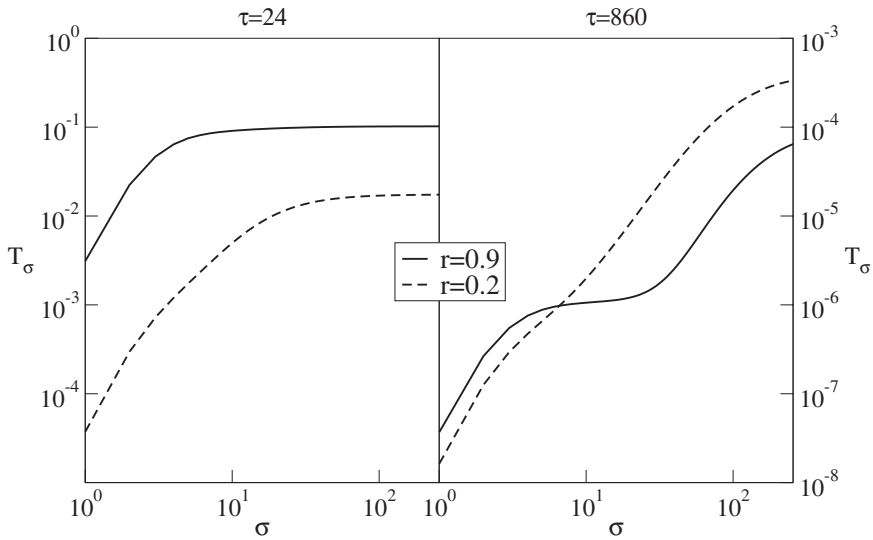


FIGURE 15 The scale-dependent temperature, T_σ , defined as function of the coarse-graining size σ for $\tau=24$ (incoherent regime) and $\tau=860$ (correlated regime for both choices of α): the system is the same as Fig. 9. In the correlated regime the more elastic case presents a plateau at intermediate wavelengths, indicating a well-defined *mesoscopic* temperature, and therefore a clear separation between the microscopic and the macroscopic scales.

we have introduced, it is possible to give an answer to such a question by defining the average local granular temperature T_σ as

$$T_\sigma = \left\langle |\mathbf{v} - \langle \mathbf{v} \rangle_\sigma|^2 \right\rangle_\sigma, \quad (35)$$

where $\langle \dots \rangle_\sigma$ means an average over a region of linear size σ .

If we call $L(t)$ a characteristic correlation length of the system, since when $\sigma \gg L(t)$ the local average, $\langle \mathbf{v} \rangle_\sigma$, tends to the global (zero) momentum, then $\lim_{\sigma \rightarrow \infty} T_\sigma = E$. For $\sigma < L(t)$, instead, $T_\sigma < E$. The behaviour of T_σ in the uncorrelated (Haff) regime and in the correlated (asymptotic) regime for two different values of α is illustrated in Fig. 15. For quasi-elastic systems T_σ exhibits a plateau for $1 \ll \sigma \ll L(t)$ that identifies the strength of the internal noise (see also the plateau in the structure factor, Fig. 12) and indicates the mesoscopic scale necessary for a hydrodynamics description. The local temperature ceases to be well defined for smaller α , leading to a scale-dependent granular temperature (Goldhirsch, 1999).

5. CONCLUSION AND PERSPECTIVES

To conclude, we have studied the kinetics of granular gases using different models and following a path of increasing complexity. The mean-field inelastic Maxwell model (or Ulam model) has an exact asymptotic solution for scalar velocities and, in general, displays power law velocity tails; however it cannot account for spatial correlations and therefore is a very poor approximation of an inelastic gas. The successive step is to

embed the same model onto a spatial lattice. In one dimension with scalar velocities, this lattice model is in a very good agreement with the kinetics of an inelastic hard rod gas. The last step of this modeling procedure is to study the lattice model in two dimensions, with vectorial velocity field. In this model, the expected asymptotic decay of the energy is reproduced and the dynamics of the growth of correlations in the velocity field is investigated by measuring the structure factors. The analysis of the structure factors and the study of other statistical properties (e.g., the distribution of the velocity gradients) indicate that the evolution of the model is consistent with that of a diffusive model with corrections due to the kinematic constraint.

This lattice model has proved to be an efficient and useful tool in the study of the cooling process in granular gases in one and two dimensions. It allows to bridge between continuum description based on the application of the Boltzmann equation and the field theoretical formulations of phase separation processes. In particular, lattice models render to manifest the role of defects during the cooling process. In one dimension such defects are shocks, in two dimensions they are shocks and vortices. It remains to be investigated which defects determine the tails of the structure functions in higher dimensions. If the leading contribution is represented by vortices, one should expect to observe $S(k) \propto k^{-d-1}$ for large values of k . Moreover, a preliminary study of an inelastic lattice mixture has revealed that the model is able to capture the phenomenon of strong deviation from equipartition.

References

- Baldassarri, A., Marini Bettolo Marconi, U. and Puglisi, A. (2001). Models of freely evolving granular gases. *Advances Complex Systems*, **4**, 321.
- Baldassarri, A., Marini Bettolo Marconi, U. and Puglisi, A. (2002b). Kinetic models of inelastic gases. *Math. Mod. Meth. Appl. S.*, **12**, 965.
- Baldassarri, A., Marini Bettolo Marconi, U. and Puglisi, A. (2002a). Influence of correlations on the velocity statistics of scalar granular gases. *Europhys. Lett.*, **58**, 14.
- Ben-Naim, E., Chen, S.Y., Doolen, G.D. and Redner, S. (1999). Shock-like dynamics of inelastic gases. *Phys. Rev. Lett.*, **83**, 4069.
- Ben-Naim, E. and Krapivsky, P. (2002). Scaling, multiscaling, and nontrivial exponents in inelastic collision processes. *Phys. Rev. E*, **66**, 011309.
- Ben-Naim, E. and Krapivsky, P.L. (2000). Multiscaling in infinite dimensional collision processes. *Phys. Rev. E.*, **61**, R5.
- Benedetto, D., Caglioti, E. and Pulvirenti, M. (1997). Kinetic equations for granular media. *Math. Mod. and Num. An.*, **31**, 615.
- Bobylev, A.V. (1975). *Proc. USSR Acad. Sci.*, **225**, 1041.
- Bray, A.J. (1994). Theory of phase ordering kinetics. *Adv. Phys.*, **43**, 357.
- Brey, J.J., Dufty, J.W., Kim, C.S. and Santos, A. (1998). Hydrodynamics for granular flow at low density. *Phys. Rev. E*, **58**, 4638.
- Brey, J.J., Moreno, F. and Dufty, J.W. (1996). Model kinetic equation for low-density granular flow. *Phys. Rev. E.*, **54**, 445.
- Das, S.K. and Puri, S. (2003). Pattern formation in the inhomogeneous cooling state of granular fluids. *Europhys. Lett.*, **61**, 749; (2003). Kinetics of inhomogeneous cooling in granular fluids. *Phys. Rev. E*, **68**, 011302.
- Ernst, M.H. (1981). Nonlinear model-Boltzmann equations and exact solutions. *Phys. Rep.*, **78**, 1.
- Ernst, M.H. (2002). Scaling solutions of inelastic Boltzmann equations with over-populated high energy tails. *J. Stat. Phys.*, **109**, 407.
- Ernst, M.H. and Brito, R. (2002). High-energy tails for inelastic maxwell models. *Europhys. Lett.*, **58**, 182.
- Espov, S.E. and Pöschel, T. (1997). *J. Stat. Phys.*, **86**, 1385.
- Frisch, U. and Bec, J. (2001). Burgulence. In: Lesieur, M., Yaglom, A. and David, F. (Eds.), *Proceedings of Les Houches 2000 New Trends in Turbulence*. Springer EDP-Science, Heidelberg.
- Goldhirsch, I. (1999). Scales and kinetics of granular flows. *Chaos*, **9**, 659.
- Goldhirsch, I. and Zanetti, G. (1993). Clustering instability in dissipative gases. *Phys. Rev. Lett.*, **70**, 1619.

- Huthmann, M., Orza, J.A.G. and Brito, R. (2000). Dynamics of deviations from the Gaussian state in a freely cooling homogeneous system of smooth inelastic particles. *Granular Matter*, **2**, 189.
- Krook, M. and Wu, T.T. (1976). Formation of Maxwellian tails. *Phys. Rev. Lett.*, **36**, 1107.
- Krook, M. and Wu, T.T. (1977). Exact solution of Boltzmann equations for multicomponent systems. *Phys. Rev. Lett.*, **38**, 991.
- Marini Bettolo Marconi, U. and Puglisi, A. (2002a). Mean field model of free cooling inelastic mixtures. *Phys. Rev. E*, **65**, 051305.
- Marini Bettolo Marconi, U. and Puglisi, A. (2002b). Steady state properties of a mean-field model of driven inelastic mixtures. *Phys. Rev. E*, **66**, 011301.
- Nakanishi, H. (2002). Velocity distribution of inelastic granular gas in homogeneous cooling state. *Phys. Rev. E*, **67**, 010301.
- Nie, X., Ben-Naim, E. and Chen, S. (2002). Dynamics of freely cooling granular gases. *Phys. Rev. Lett.*, **89**, 204301.
- Ostojic, S., Panja, D. and Nienhuis, B. Clustering in a one-dimensional inelastic lattice gas. cond-mat/0310493, to appear in *Phys. Rev. E*.
- Pöschel, T., Brilliantov, N.V. and Schwager, T. (2002). Violation of molecular chaos in dissipative gases. *Int. J. Mod. Phys. C*, **13**, 1263.
- Pöschel, T. and Luding, S. (2000). *Granular Gases*. Springer Verlag, Berlin.
- Porod, G. (1951). Die Röntgenkleinwinkelstreuung von dichtgepackten kolloiden systemen. *Kolloid Z.*, **124**, 83.
- Ulam, S. (1980). On the operations of pair production, transmutations and generalized random walk. *Adv. Appl. Math.*, **1**, 7.
- van Noije, T.P.C., Ernst, M.H., Brito, R. and Orza, J.A.G. (1997). Mesoscopic theory of granular fluids. *Phys. Rev. Lett.*, **79**, 411.
- van Noije, T.P.C. and Ernst, M.H. (1998a). Ring kinetic theory for an idealized granular gas. *Physica A*, **251**, 266.
- van Noije, T.P.C. and Ernst, M.H. (1998b). Velocity distributions in homogeneous granular fluids: the free and the heated case. *Granular Matter*, **1**, 57.
- Vicente Garzó and James Dufty (1999). Homogeneous cooling state for a granular mixture. *Phys. Rev. E*, **60**, 5706.